A novel protein from the serum of Python sebae, structurally homologous to γ-phospholipase A2 inhibitor, displays antitumor activity

Sandra Donnini, Federica Finetti, Simona Francese, Francesca Boscaro, Francesca Dani, Fabio Maset, Roberta Frasson, Michele Palmieri, Mario Pazzagli, Vincenzo de Filippis, et al.

A novel protein from the serum of Python sebae, structurally homologous to γ-phospholipase A2 inhibitor, displays antitumor activity

Sandra Donnini*, Federica Finetti*, Simona Francese[†], Francesca Boscaro[‡], Francesca Romani Dani[‡], Fabio Maset[§], Roberta Frasson[§], Michele Palmieri*, Mario Pazzagli[¤], Vincenzo De Filippis[§], Enrico Garaci[¶], and Marina Ziche*

[*]Department of Biotechnology, and Istituto Toscano Tumori (ITT), University of Siena, Via A. Moro 2, 53100 Siena, [†]Biomedical Research Centre, Sheffield Hallam University, Howard Street, S1 1WT Sheffield, UK, [‡]Mass Spectrometry Center (C.I.S.M.), Viale Pieraccini 6, 50139 Florence, [§]Department of Pharmaceutical Sciences, University of Padua, Via F. Marzolo 5, 35130 Padua; [¤]Department of Clinical Physiopathology, University of Florence, Viale Pieraccini 6, 50139 Florence; [¶]Department of Experimental Medicine and Biochemical Sciences, University of Rome "TorVergata" Viale Regina Elena, 299, 00133, Rome.

Short Title: Cytotoxic activity of a novel serum protein of Python sebae

Corrispondence to: Marina Ziche MD, Department of Molecular Biology, University of Siena, Via Aldo Moro 2, 53100 Siena, Italy. Phone +39-0577-234444, Fax +39-0577-234343 E-mail: ziche@unisi.it

Synopsis

Cytotoxic and antitumors factors have been documented in the venom of snakes, while little information is available on the identification of cytotoxic products in the snake serum. In this study, we purified and characterized a new cytotoxic factor from serum of the non venomous *Phyton sebae*, endowed with antitumor activity. The serum of the *P. sebae*, termed PSS, exerted a cytotoxic activity and reduced dose dependently the viability of several different tumor cell lines. In a model of human squamous cell carcinoma xenograft (A431), subcutaneous injection of PSS in proximity of the tumor mass reduced by 20% tumor volume. Fractionation of PSS by ion-exchange chromatography yielded an active protein fraction, F5, which significantly reduced tumor cell viability in vitro, and strikingly tumor growth in vivo. F5 is composed of P1 and P2 subunits interacting in a 1:1 stoichiometric ratio to form a hetero-tetramer in equilibrium with a hexameric form, which retained the biological activity only when assembled. The two peptides share sequence similarity with type-γ phospholipase A2 (PLA2) inhibitor (PLI-γ) from *P. reticulatus*, PIP, existing as a homo-hexamer. More importantly, while PIP inhibits the hydrolytic activity of PLA2, the anti-PLA2 function of F5 is negligible. Using high resolution mass spectrometry, we covered 87 and 97% sequence of P1 and P2. In conclusion, here we have identified and thoroughly characterized a novel protein displaying high sequence similarity with PLI-γ molecule and possessing remarkable cytotoxic and antitumor effects, that can be exploited for potential pharmacological applications.

Key words: snake serum, antitumor activity, type-γ phospholipase inhibitor, apoptosis, Phyton sebae.

Introduction

Little information is available on the identification of antitumor products in the snake serum, [1]. On the contrary, a variety of factors with cytotoxic activity against murine and human tumor cell lines *in vitro*, and antitumor efficacy *in vivo* have been documented in the snake venom and several proteins, including proteases and phospholipases (PLA2s), have been isolated and characterized [2-7]. To protect themselves from leakage of their own venom PLA2s into the circulatory system, venomous snakes contain in their blood PLA2s inhibitors (PLIs), classified into three groups according to their structure and selectivity for specific PLA2s groups (i.e., PLIα, PLIβ and PLIγ) [8,9]. PLIs are acidic oligomeric glycoproteins with N-linked oligosaccharide chains, composed of three to six identical or different non-covalently linked subunits having a molecular weight of 20-30 kDa [10,11]. PLIα is a trimer composed of identical 20 kDa subunits, having a C-type lectin domain, and specifically inhibits group-II acidic PLA2s. PLIβ selectively inhibits group-II basic PLS2s and has nine tandem leucine-rich repeats in its sequence. Contrary to PLIα and PLIβ, PLIγ is a rather nonspecific inhibitor and its primary structure is characterized by two tandem patterns of Cys-residues, as are found in urokinase-type plasminogen activator receptor and in Ly6-related proteins [8,10,12]. All three types of PLIs have been found in the sera of both venomous snakes like *Viperidae* [11] and nonvenomous snakes like *Elaphe quadrivirgata* [13] and *Python reticulatus* [14]. Thus, the presence of PLIs in nonvenomous snakes suggest that their physiological role might not be restricted to the protection against the venom PLA2s, and that PLIs may exhibit other different, still unknown, functions.

In this study we have sampled sera from the non-venomous snake African Rock Python (*P. sebae*), and tested on several assays for cell toxicity and viability, and on in vivo tumor growth. We show that the serum from the non-venomous snake *P. sebae* (PSS) produces cytotoxic and antiproliferative effects on tumor cells growing *in vitro* and reduces tumor growth in nude mice transplanted with A431 tumor cell without side effects. To identify the chemical component(s) responsible for the cytotoxic and antitumor activity, PSS was fractionated by ion-exchange chromatography, yielding an active protein fraction (i.e., F5). F5 reduced tumor cell viability *in vitro*, by inducing apoptosis with a mechanism involving activation of caspase-3, and *in vivo,* inhibited A431 xenograft growth in nude mice. Notably, size-exclusion chromatography and dynamic light scattering measurements revealed that F5 is composed of P1 and P2 subunits interacting in a 1:1 molar ratio to form a tetrameric structure in equilibrium with a hexameric form. Isolated P1 and P2 lack cytotoxic and antitumor effects. *De novo* sequencing of P1 and P2 reveal that these subunits display high sequence similarity with type-γ PLI from *P. reticulatus*, PIP [14]. Conversely to PIP, however, F5 was unable to inhibit PLA2s.

In conclusion, here we have identified and thoroughly characterized a novel protein displaying high sequence similarity with PLI-γ molecule and possessing remarkable cytotoxic and antitumor effects, that can be exploited for potential pharmacological applications.

Material and Methods

Python serum sampling

Serum from the African Rock Python specie (*P. sebae*, species sebae sebae) was sampled from two females aged approximately three years. As a control, serum was also sampled from two females of the *P. regius* specie, aged approximately three and four years. All donor snakes were born in captivity. In animal starved for 24 h and sedated by gentle handling for 2 h, blood samples (average 10 ml) were withdrawn from the cardiac cavity by a 20 cc syringe with a 21G needle. After sedimentation and centrifugation at 3000 rpm at room temperature for 10 min, the clear supernatant was removed and stored in aliquots at –20°C and used as such in the experiments after proper dilution in culture media or PBS. In the experiments the serum was diluted in culture medium deprived of FCS, and titration was performed by protein content quantified by the Bradford assay. The *P. sebae* serum is identified all through the manuscript by the abbreviation PSS, while *P. regius* serum is identified as PRS.

Functional assays

Cells and culture conditions. Human squamous epithelial carcinoma (A431), human glioblastoma (U373 MG), human breast cancer (MCF-7) cell lines and human fibroblast (HF) cell line were from the American Type Culture Collection (ATCC). The A431 and MCF-7 cell line were cultured in DMEM with 4500 mg/L of glucose and 10% fetal calf serum (FCS). HF cell line was cultured in DMEM with 1000 mg/L of glucose, 1% non essential aminoacids, 10% sodium pyruvate and 10% FCS. U373 MG cell line was cultured in MEM with 1% non essential aminoacids, 10% sodium pyruvate and 10% FCS. Mouse lung carcinoma cell line (LLC) was kindly provided by Dr. F. Pica at the University of Tor Vergata, Rome, and were cultured in RPMI 1640 with 10% FCS. Capillary venular endothelial cells (CVEC) were obtained and cultured as described [10].

MTT assay. Cell survival was quantified as described [15,16], by Vybrant MTT cell assay kit (Molecular Probe). Briefly, cells (2 x 10^3 cells/well for CVEC and FU or 3 x 10^3/well for A431, MCF-7 and U373MG) were seeded in 96 well microtiter plate with medium containing 10% FCS for 5 h, stabilised in 0,1% FCS for 16 h. Cells were then exposed to different concentrations of PSS for 5 days or to PSS fractions (F1 to F6) for 48 h, in media with 1% FCS. After incubation cultures were washed with PBS and incubated for 4 h with 1.2 mM MTT (3-(4,5-dimethylthiazol-2-yl)-2,5-diphenyltetrazolium bromide) in fresh medium. Culture medium was then replaced with equal volume of DMSO to dissolve formazan crystals. The absorbance of the formazan was measured with a microplate absorbance reader (Tecan) at 540 nm. The cell survival was reported as % cell viability. Percent cell viability = (absorbance experimental wells x 100)/(absorbance basal wells).

Apoptosis and necrosis analysis. Bivariant flow cytometry was performed on adherent cells grown in the presence or absence of PSS for 4 h in media containing 1% FCS. After incubation, cells were washed in cold PBS and resuspended in 100 µl of binding buffer (HEPES containing 2.5 M $CaCl_2$). Fluorescein-labeled Annexin V and propidium iodide (PI) were added to the cell suspension. Annexin V, a member of the calcium and phospholipids-binding proteins, binds strongly and specifically to phosphatidylserine which is a marker of cell apoptosis, while PI binds cell DNA, highlighting necrotic cells. Cells were then analysed by flow cytometry (Becton Dickinson, USA) and the results are expressed as % of positive cells/total cells.

In vivo tumor growth. Animal studies were carried out according to the European Economic Community for animal care and welfare (EEC Law No. 86/609), using female 5 week-old Balb/c nude mice (Harlan Nossan) housed in a barrier care facility and caged in groups of six [17]. Mice were implanted subcutaneously with A431 (10 x 10^6) cells resuspended in 100 µl of sterile PBS. After 4 days, when the diameter of tumor mass ranged between 0.5 and 1 mm^3, mice were treated every other day with 100 µl of a solution containing 100 µg PSS (six mice) or F5 (50 µg/mouse, six mice), injected subcutaneously in proximity of the tumor mass for 12 days. Control mice were treated with PBS (six mice), or with F3 (50 µg/mouse, six mice). Mice were assigned randomly to

either group. Tumor dimensions were measured every two days with a calliper. Tumor volumes were calculated by taking width x length x thickness. The survival time of mice was also recorded.

Western Blotting

Cells (3 x 10^5) were seeded in 60 mm diameter dishes. After adherence, cells were serum starved (0.1% serum, 24 h) and then stimulated with F1 or F5 (5 ug/ml) in 1% FCS. Cells were then lysed and centrifuged at 10000 g (20 min at 4°C). 30 µg of proteins were mixed with 4X reducing SDS-PAGE sample buffer and denatured (10 min at 100°C). Anti-cleaved-caspase-3 antibody was used (1:1000, Santa Cruz). Results were normalized with actin (1:10000).

Phospholipase A2 activity assay

The secretory PLA2 (sPLA2) activity was measured by using the sPLA2 Assay Kit (Cayman). Briefly, 10^6 A431 cells/100 mm dishes were plated in 10% FCS for 24 h and then the conditioned medium was collected, concentrated by Amicon Concentrator columns (cut off 3 kDa) and tested for secretory Phospholipase A2 (PLA2) activity in the presence or absence of F5 or F1 following manufactures instructions.

The inhibitory activity of PSS or its fractions was assayed by the sPLA2 (type V) Inhibitor Screening Assay kit (Cayman). Briefly, different concentrations of PSS or its cytotoxic fractions were added to the plate containing the sPLA2 and the inhibitory activity evaluated as absorbance at 405 nm after 1 minute using a plate reader. Data are reported as % inhibition for each sample versus sPLA2 activity.

Statistics

Results are expressed as means ± SD. Statistical analysis were performed using Student's t-test. Differences between groups were considered statistically significant at $p<0.05$.

Fractionation of PSS

Anion exchange chromatography. PSS (100 µl) diluted 1:5 in 20 mM Tris-HCl, pH 7.5, 0.15 M NaCl, was fractionated by ion-exchange chromatography on a FPLC system, by using a 6 x 60 mm MonoQ (Amersham-Pharmacia Biotech) anion exchange column. The serum diluted in Tris-HCl buffer was centrifuged for 2 min at 13000 rpm, filtered at 0.45 µm on a miniclarifying filter (Millipore), and then applied to the column. The column was equilibrated in 20 mM Tris-HCl pH 7.5, containing 0.15 M NaCl at a flow rate of 0.5 ml/min, and eluted with a linear gradient of NaCl from 0.15 to 1.0 M. The absorbance of the effluent was monitored at 280 nm.

Determination of total protein concentration. The protein material eluted in correspondence of the chromatographic peaks were collected and the protein content was estimated by the method of Bradford and that of bicinchoninic acid (BCA). Aliquots of these fractions were tested for cytotoxic and antitumor activities as described above.

RP-HPLC. The fractions eluted at 0.4 M NaCl concentration, denoted as F5 and deriving from several different chromatographic runs, were pooled and lyophilised. An aliquot (about 50 µg) of these fractions were successively solubilized in 0.5 ml of aqueous trifluoroacetic acid (0.1% TFA) and purified, as described by RP-HPLC, on a C4 analytical column from Vydac (The Separation Group, Hesperia, CA) (4.6 x 150 mm, 5 µm particle size). The column was equilibrated with aqueous 0.1% TFA and eluted with a linear acetonitrile-0.1% TFA gradient from 30 to 60 % in 35 minutes, at a flow rate of 0.8 ml/min. The absorbance of the effluent was recorded at 226 nm. The presence of two peaks was observed, eluted at about 19 and 25 minutes, denoted as P1 and P2. These fractions were lyophilised and subjected to subsequent analyses.

Chemical characterization

Analytical size-exclusion chromatography of F5. The apparent molecular weight of fraction F5 eluting at 0.4 M NaCl from the ion exchange column, was determined by analytical gel filtration chromatography. Samples were loaded onto a Superose-12 column (1 x 30 cm, Amersham-Pharmacia Biotech), and eluted with 20 mM Tris/HCl buffer, pH 7.5, at a flow rate of 0.3 ml/min. The column was calibrated using a protein mixture of known molecular weight, in the range of 6.5 – 135 kDa: bovine serum albumin (67 kDa), ovalbumin (43 kDa), charbonic anydrase (29 kDa), Ribonuclease A (13.7 kDa) and aprotinin (6.5 kDa). The interstitial volume (V_i) and the void volume (V_0) were determined by loading the Gly-Tyr-Gly tripeptide and dextran blue (2000 kDa), respectively. The distribution constant (K_D) value was calculated by the equation $K_D = (V_e - V_0)/(V_i - V_e)$, where V_e was the elution volume of the proteins loaded onto the column.

Dynamic light scattering of F5. Dynamic light scattering (DLS) measurements on F5 samples (0.7 mg/ml solution filtered at 0.22 μm cutoff) were carried out at 25±0.1°C with a Zetasizer Nano S (Malvern Instruments, U.K.) at a fixed angle (i.e., 173°) from the incident light (i.e., a He-Ne 4 mW power laser source at 633 nm). ZEN-0117 1-cm pathlength polystyrene cuvettes (100 μl) (Hellma Italia, Milan, Italy) were used for all measurements. Each measurement consisted of a subset of runs automatically determined, each being averaged for 10 s. Scattering data were analysed with the multimodal alogorithm, as implemented in the Nano vs. 6.20 software, and presented as the per cent volume size distribution. The refractive index (n) and viscosity (η) of the protein solutions were taken as 1.330 and 0.887 cP.

Electrophoresis. Protein fractions were analysed by gradient gel electrophoresis (SDS-PAGE) using 4-12% polyacrylamide precast gels. Lyophilized fractions from anion exchange chromatography were diluted in 20 μl gel loading buffer. Samples were then loaded onto the gel, which was run in Tris-glycine buffer, pH 8.3, with 0.1% SDS. After SDS-PAGE, protein bands were stained by immersing the gel in 0.1% Coomassie blue solution in water/methanol/acetic acid (5:4:1) for 30 min and destaining by several changes in 40% methanol, 10% acetic acid until clear background was obtained. To possibly identify carbohydrate chains, protein bands were stained with the GelCode Glycoprotein Staining Kit (Pierce chem Co.), according to the manufacture's procedures.

Mass spectrometry and data analysis. For MALDI-TOF-TOF analyses, 1 μl of proteolytic digest was deposited on an AnchorChip™ target plate (Bruker Daltonics, Bremen, Germany) and allowed to dry; 0.35 μl of matrix (α-cyano-4-hydroxycinnamic acid 5g/l in 50/50 acetonitrile/0.1% TFA) were then added and, again, allowed to dry. Mass spectrometric (MS) analysis was performed on an Ultraflex III MALDI-TOF-TOF (Bruker Daltonics, Bremen, Germany) by using the Flex Control™ 3.0 data acquisition software. Mass spectra were acquired in reflectron mode over the m/z range 800-5000. The instrumental parameters were chosen by setting the ion source at 25 kV, the reflector at 26.30 kV and the delay time at 20 ns. The instrument was externally calibrated prior to analysis by using the Bruker peptide calibrant kit (1046-3147 Da) and the sample spectra internally recalibrated with trypsin autolysis signals. For MS data acquisition, a total of 400 shots were collected. The peptide masses present in each mass spectrum, through the integrated software Biotools™ 3.0, are used to search the NCBInr databank. Fragmentation of tryptic peptides was obtained using the LIFT™ technology (Bruker Daltonics).

For LC-MS analyses, a Mariner ESI-TOF instrument (Perseptive Biosystems, Stafford, TX) was used. Spray Tip Potential was set at 3.0 kV, the nozzle potential and temperature at 200 Volts and temperature were set at 140°C, respectively. Alternatively, MS/MS analyses were carried out with an Ultimate 3000 (LC Packings Dionex, San Donato Milanese, Milano, Italy) coupled with an LTQ Orbitrap mass spectrometer (Thermo Fisher, Bremen, Germany). Peptides were first concentrated on a precolumn cartridge PepMap100 C18 (300 μm×5mm, 5μm granulometry, 100Å porosity) from

LC Packings Dionex and then eluted on a C18 PepMap100 column (75µm×15cm, 5µm granulometry, 100Å porosity) from LC Packings Dionex at a flow rate of 300 nL/min. The mobile phases composition was: H_2O 0.1% formic acid/CH_3CN 97/3 (phase A) and CH3CN 0.1% formic acid/H_2O 97/3 (phase B). The gradient program was: 0 min, 4% B; 10 min, 40% B; 30 min, 65% B; 35 min, 65%B; 36 min, 90% B; 40 min, 90% B; 41 min, 4% B; 60 min, 4% B. Mass spectra were acquired in the positive ion mode, setting the spray voltage at 1.9 kV, the capillary voltage and temperature respectively at 40 V and 200 °C, and the tube lens at 130 V. Data were acquired in data dependent mode with dynamic exclusion enabled (repeat count 2); survey MS scans were recorded in the Orbitrap analyzer in the mass range 300-2000 m/z at 15.000 nominal resolution, then up to three most intense ions in each full MS scan were fragmented and analyzed in the Orbitrap analyzer at a 7.500 nominal resolution. Singly charged ions did not trigger MS/MS experiments. The acquired data were searched using Bioworks 3.2 (Thermo Fisher) using Sequest as search algorithm against all the sequences reported in Uniprot for taxon Python and adding new sequences containing the modifications identified during LIFT experiments. S-carbamidomethylation or S-pyridylethylation was selected as complete modification; two missed cleavages were allowed for trypsin chosen as cleaving agent. Searches were performed with a tolerance of 10 ppm.

N-Terminal Sequence analysis. The first twelve amino acids of purified fractions (P1 and P2) were determined by Edman degradation, carried out by PRIMM (Biotech Products and Services, Milan, Italy) using an automatic protein sequencer mod. 477-A (Applied Biosystems, Foster City, CA).

Determination of the cysteine content. Aliquots (100 µg) of RP-HPLC purified P1 and P2 fractions were subjected to reduction of disulfide bonds and carboxaamidomethylation reaction of the cysteine (Cys) residues, eventually present along the amino acid sequence, to yield the corresponding S-carboxamidomethylated (S-CM) derivatives. The reduction reaction was conducted at 37°C in 0.1 M Tris/HCl buffer, pH 7.8, 1 mM EDTA and 0.125 M dithiothreitol (DTT). After 2-h reaction, iodoacetamide was added up to a final concentration of 0.25 M and the reaction allowed to proceed for 90 minutes at 37°C. The reaction mixture was then fractionated by RP-HPLC on a C4 analytical column (4.6 x 150 mm, 5 µm particle size), equilibrated with 0.1% aqueous TFA and eluted with a linear acetonitrile-0.1% TFA gradient from 30 to 60% in 35 min, at a flow rate of 0.8 ml/min. Alternatively, P1 and P2 (100 µg each), with Cys-residues in the reduced state, were treated for 90 min at 37°C with 4-vinylpyridine (4VP) (0.25 M) to yield the corresponding S-pyridylethylated (S-PE) derivatives. The reaction was fractionated by RP-HPLC on a C3 (4.6 x 150 mm, 5 µm particle size) analytical column (Agilent Technologies), eluted with a linear acetonitrile-0.1% TFA gradient from 10 to 30% in 5 minutes and from 30 to 60 % in 40 minutes, at a flow rate of 0.8 ml/min. The absorbance of the effluent was recorded at 226 nm.

Deglycosylation reaction. 20 µg of purified P1 or P2 were dissolved in 200 µl of 20 mM sodium phosphate buffer, pH 7.2, containing 100 mM EDTA, 1% (by vol.) β-mercaptothanol. This solution was treated for 24 hours at 37°C with N-glycosidase F (Roche) (0.2 U of enzyme per mg of protein). The reaction mixture was fractionated by RP-HPLC and analysed by SDS-PAGE. The polyacrylamide gel was stained either with Coomassie or with the GelCode Glycoprotein Staining Kit.

Disulfide reduction and cysteine derivatization of P1 and P2. Reduction of protein (10 µg) disulfide bonds was carried out under denaturing conditions in 0.125 M Tris–HCl buffer, pH 8.3, containing 1mM EDTA and 6 M guanidinium hydrochloride (Gnd-HCl) in the presence of 50-fold molar excess of DTT over the total cysteine content and incubation was conducted at 56 °C for 90 min. Iodoacetamide was then added in a 10-fold molar excess over the total cysteine content, and the mixture was further incubated in the dark for 60 min at 37 °C. Desalting was carried out on a

PD-10 column (GE Healthcare Bio-Sciences, Uppsala, Sweden), eluted in 40 mM ammonium bicarbonate buffer. Four 0.5-ml fractions were collected, lyophilised in a SpeedVac (Thermo, San Josè, CA) concentrator and finally dissolved in 40 µl of 50 mM ammonium hydrogen bicarbonate, pH 7.0. Alternatively, P1 and P2 (100 µg each), with Cys-residues in the reduced state, were treated for 90 min at 37°C with 4-vinylpyridine (4VP) (0.25 M) to yield the corresponding S-pyridylethylated (S-PE) derivatives. The reaction was stopped by addition of 1 M citric acid solution down to pH 4, and fractionated by RP-HPLC on a C3 (4.6 x 150 mm, 5 µm particle size) analytical column from Agilent Technologies. The column was eluted with a linear acetonitrile-0.1% TFA gradient from 10 to 30% in 5 minutes and from 30 to 60 % in 40 minutes, at a flow rate of 0.8 ml/min. The absorbance of the effluent was recorded at 226 nm.

Tryptic digestion of S-carboxamidomethylated (S-CM-P1 S-CM-P2) or S-pyridylethylated (S-PE-P1 and S-PE-P2) P1 and P2 subunits. Derivatised proteins (100 µg) were dissolved in 50 mM Tris-HCl, pH 8.0, 1 mM $CaCl_2$ (200 µl). To this solution, sequencing grade trypsin (Promega) was added to a final enzyme:protein ratio of 1:20 (w/w). The reaction mixture was incubated at 37°C overnight, stopped by adding 50 µl of 20% aqueous formic acid, and fractionated by RP-HPLC on a C18 analytical column (Agilent Technologies) eluted at a flow rate of 0.8 ml/min with a linear acetonitrile-0.1% TFA gradient from 5 to 50 % in 40 minutes. The absorbance of the effluent was recorded at 226 nm. Peptide material eluted in correspondence of the chromatographic peaks were collected, lyophilised, and dissolved in 1%-aqueous formic acid for subsequent mass spectrometry analysis. Cys-containing fragments were identified by spectrophotometric analysis of S-pyridylethylated cysteine in the near-UV region (350-240 nm), using a model Lambda 2 Perkin-Elmer (Norwalk, CA) UV-Vis spectrophotometer

Subdigestion of tryptic fragments with leucine aminopeptidase (LAP). P2 tryptic digest was dried in a SpeedVac concentrator and then dissolved in 12 µl of 20 mM Tris-HCl buffer (pH 7.5) containing 1 mM $MgCl_2$. Five microliters of this solution were added to 1 µl of LAP (30 units/µl) (Sigma-Aldrich) at room temperature. Aliquots (1 µl) were withdrawn after 1, 2 and 5 min, and anlysed by MALDI-TOF or ESI-TOF.

Subdigestion of tryptic fragments with Glu-C endoproteinase. Tryptic fragments that remained unidentified in LC-MS analysis, were lyophilised, dissolved in 100 µl of sodium phosphate buffer, pH 7.8, and treated at 37°C for 2 hours with Glu-C endoproteinase V8 from *S. aureus*, using a peptide:protease ratio of 1:50 (w/w). The reaction was stopped by acid addition and analysed by RP-HPLC on a C18 (4.6 x 150 mm) column eluted with a linear acetonitrile-0.1% TFA gradient from 2 to 60% in 10 minutes.

Digestion of S-PE-P1 and S-PE-P2 with Glu-C endoproteinase. Aliquots (100 µg) of derivatised P1 or P2 were dissolved in sodium phosphate buffer, pH 7.8 (200 µl). To this solution, Glu-C endoproteinase V8 (Boheringher) was added to a final enzyme:protein ratio of 1:20 (w/w). The reaction mixture was incubated at 37°C overnight, stopped by adding 50 µl of 20% aqueous formic acid, and fractionated by RP-HPLC. The chromatographic peaks were lyophilised, dissolved in 1% aqueous formic acid and analysed by ESI-TOF mass spectrometry. Prior to mass analysis, all chromatographic fractions were scanned by UV-Vis absorption spectroscopy for identifying S-pyridylethylated Cys-residues.

Spectroscopic measurements

Protein concentration was determined by the method of bicinconinic acid for both P1 and P2 recording the absorbance of the solution at 562 nm on a double beam model Lambda-2 spectrophotometer from Perkin-Elmer (Norwalk, CT). Circular dichroism (CD) spectra were recorded on a Jasco (Tokyo, japan) model J-810 spectropolarimeter equipped with a thermostated

cell-holder connected to a NesLab (Newington, NH) model RTE-111 water-circulating bath. Far-UV CD spectra were recorded at 20 ± 0.5°C in 10 mM sodium phosphate pH 7.0, using a 1-mm pathlength quartz cell.

Results

PSS induces cytotoxicity in tumor and non tumor cell lines

Cytotoxicity was evaluated in cell suspension as well as on adherent cells. Exposure to PSS in the 50-2000 µg/ml range, induced concentration-dependent cytotoxicity in human tumor cell lines (A431 and U373MG, ED50 = 125 µg/ml; MCF-7, ED50 = 200 µg/ml), in mouse tumor cell line (LLC, ED50 = 150 µg/ml) and in the non-tumor cell lines bovine endothelial cells (CVEC, ED50 = 230 µg/ml) and human skin fibroblasts (HF, ED50 = 250 µg/ml). (Table S1A and B). To investigate the species specificity of PSS activity we assessed the effect of the serum obtained from two specimens of *P. regius*, PRS1 and PRS2, and from another specimen of the African Rock Python, PSS2. Similar results were obtained with PSS2, while PRS1 and PRS2 failed to induce cytotoxic effects (Table S2).

PSS reduces cell viability

Microscope observation of cells stained with Diff Quick after 1 h exposure to PSS (200 µg/ml) showed that the cytotoxicity was mainly characterized by retraction of cytoplasmic expansion, leading to round shaped cells and lysis of cell bodies when compared to basal condition (1% FCS without PSS) (Fig. S1). Then, the PSS effects on cell viability were investigated using the MTT assay. Cells were exposed to PSS for 5 days at concentrations selected as the least toxic, based on previous results. Exposure to repeated PSS treatment (every 2 days for 5 days) in the low concentration range (20-100 µg/ml), evidenced that PSS at 20 µg/ml had no relevant effect on cell viability for any cell line. However, at higher concentrations, PSS significantly and concentration-dependently reduced cell viability (Fig. 1).

PSS induces cell apoptosis and necrosis

As reported in Fig. S1, microscope observations of cells stained with Diff Quick, following PSS treatment documented that changes were compatible with the occurrence of cell apoptosis and necrosis (retraction of cytoplasmic expansion, rounding of cell shape and lysis of cell bodies). To further investigate the PSS toxic mechanism and to corroborate the hypothesis that cytotoxicity was mainly associated with cell apoptosis and necrosis, we performed apoptosis/necrosis studies by bivariant flow cytometry analysis using fluorescein-labelled annexin V and propidium iodide (PI) stained cells. In Table 1 are reported the flow-cytometry results of the tumor cell lines A431 and U373MG exposed to different PSS concentrations for 4h. At the maximal PSS concentration tested (200 µg/ml), about 50% of cells were positive for PI, and 30 % were positive for Annexin V.

PSS reduces *in-vivo* tumor growth

We investigated the effect of PSS treatment on solid tumor growth and overall survival in nude mice. The short supply of test compound, limited the number of animals entering the study. A431 cell line was selected for in vivo experiments. Once A431 cells had produced palpable tumors (4 days after subcutaneous transplant of cells) with tumor mass ranging between 0.5 and 1 mm^3, treatment with subcutaneous PSS in proximity of the tumor mass was started with a dosing schedule of 100 µg every other day for 12 days. A total of 7 treatments was performed. Six control mice, bearing similar tumor masses, were treated with sterile PBS only. PSS treatment was well tolerated, producing neither local nor systemic effect. An additional group of mice which received PSS by intra-peritoneal injection survived the treatment with no apparent toxic effect (data not shown). PSS treatment reduced A431 tumor growth, and after one week, the tumor volume compared to control was reduced by 20% (days 11 and 13 of Fig. 2, $P<0.05$). PSS treatment also affected survival, as 4 out of 6 mice survived at day 21 whereas none of the control survived. However, given the small number of animals, this difference did not reach significance (data not shown).

Fractionation of PSS and functional characterization of the active component F5

To purify and further characterize the active component(s) triggering cell death, PSS was fractionated by anion-exchange chromatography (Fig. 3A) on a Mono-Q column. Aliquots of the protein fractions were analysed by reducing SDS-PAGE (see Inset to Fig. 3A). Fraction F2 contains a minor component at 75 kDa, while F3 contains the major component, migrating at 67 kDa, likely corresponding to the snake albumin. Fraction F4 is contaminated by F3 and contains two additional bands at 48 and 35 kDa. Of note, fraction F5 eluting at 0.43 M NaCl contains a highly homogeneous component at about 23 kDa. The concentration of eluted fractions was determined by the BCA assay (see Methods) and the effect of each fraction (50 µg/ml, final assay concentration) on cell viability was evaluated using A431, MCF-7 and U373MG tumor cell lines.

As deduced from TB and MTT proliferation assays (Fig. 3B), only F5 retained the cytotoxic and anti-proliferative effect of PSS. We then assessed the effect of F5 on A431 xenograft in nude mice. We compared the antitumor efficacy exerted by F5 (50 µg/100 µl/mouse) with that obtained by administration of F3 or with PBS (100 µl/mouse, Control). Tumor growth in the control (Ctr) or F3 treated group proceeded steadily from day 5 increasing up to day 12. Conversely, in animals receiving F5, tumor mass was reduced by approximately 60% (Fig. 3C, $P<0.05$). In the experimental time frame adopted, neither mortality nor weight loss were observed in any groups.

Further, we investigated the ability of F5 to affect caspase-3 activation, phosphatidylserine expression, and tubulin assembly. As shown in Fig. 4 and Fig S2, the cellular effects of F5 appeared to be linked to induction of cell apoptosis, as indicated by caspase-3 activation and phosphatidylserine expression in A431 (Fig. 4A and B). Conversely, no effect was detected on tubulin assembly, as assessed by immunofluorescence in CVEC, A431 and U373MG cells exposed for 24 h to F5 (50 µg/ml) or, as positive control, to colchicin (25 µg/ml) (Fig. S2).

Chemical characterization of the active component F5

Further fractionation of F5 by RP-HPLC (Fig. 5A) on a C4 analytical column yielded two chromatographic peaks of comparable intensity, denoted as P1 and P2, and having molecular mass values of 23135 ± 2 u.m.a. and 23152 ± 2 u.m.a., respectively. This small mass difference is consistent with the fact that P1 and P2 of F5 migrate as a single band in SDS-PAGE (see Fig. 3A, Inset). Notably, when tested for biological activity, either P1 and P2 revealed complete loss of cytotoxic activity (data not shown).

Deglycosylation of disulfide-reduced P2 with N-glycosidase F, which hydrolyses N-linked glycosylation sites at asparagine residues, resulted in a species at 20290.06 ± 5 a.m.u., indicating that the mass contribution of the carbohydrate chain(s) is 2862 a.m.u.. In the case of P1, treatment with N-glycosidase F resulted in the precipitation and loss of the protein sample.

The glycoprotein nature of P1 and P2 was confirmed by staining the electrophoretic gel with Coomassie R-250 and with the glycoprotein specific GelCode staining kit before and after treatment with N-glycosidase F. As expected, P1 and P2 bands normally stain blue with Coomassie, regardless glycosidase treatment. Notably, only untreated P1 and P2 stain pink with the GelCode. In agreement with MS data, deglycosylated P1 and P2 bands migrate in SDS-PAGE with a molecular weight 2-3 kDa lower than that of intact proteins (not shown).

Determination of Cys-content of P2 fraction was carried out by reduction/carboxamidomethylation reaction with DTT/iodoacetamide. The Cys-reduced and carboxamidomethylated P2 (S-CM-P2) eluted as a single peak in RP-HPLC on a C4 analytical column (not shown), with an increase in the mass value of 928.9 ± 0.4 a.m.u. Considering that carboxamidomethylation of half-cystine adds 58.03 a.m.u, we conclude that P2 contains 16 cysteines (16 x 58.03 a.m.u. = 928.48 a.m.u.). Of note, neither P1 nor P2 reacts with Ellman's reagent (dithio-bis(2-nitrobenzoic acid), indicating that no free Cys-residues is present. Similar results were obtained either with P1 and P2, after reduction and derivatization with 4-vinylpyridine, a more selective reagent for Cys-residues [18]. In both cases, a mass increment of 1696 ± 0.7 a.m.u. was obtained, thus confirming the presence of 16 cysteines in both proteins (106 a.m.u. x 16 = 1696 a.m.u.), arranged to form eight disulfide bonds.

Quaternary structure of the active component F5

As mentioned above, RP-HPLC analysis of F5 shows the presence of two peaks (i.e., P1 and P2) of similar height and area, suggesting that they are represented in F5 in a 1:1 ratio (Fig. 5A). However, to discriminate whether P1 and P2 simply co-elute in the F5 fraction during ion-exchange chromatography (Fig. 3A) or if they are constitutively associated in F5 to form an oligomeric complex, analytical size-exclusion chromatography (SEC) (Fig. 5B) and dynamic light scattering (DLS) (Fig. 5C) techniques were used. The SEC trace indicate that F5 is conformationally heterogeneous, with a minor species eluting with the void volume, likely corresponding to a high molecular weight protein aggregate, and a predominant species eluting with an apparent molecular weight of 87 ± 10 kDa, likely corresponding to a tetramer. A third species elutes as a shoulder with an apparent molecular weight of 123 ± 20 kDa, possibly corresponding to a hexameric form. However, SEC analysis implies dilution of the sample which can complicate the data interpretation, as concentration-dependent dissociation of the subunits can occur [19].

To overcome this problem, we conducted DLS measurements, where there is no need of sample dilution. In DLS analysis the time dependent fluctuations of scattered light from molecules of different size in solution is measured and the rate of these fluctuation is inversely correlated with the molecule size. Generally, an increased hydrodynamic radius (R_H) is obtained for elongated molecules compared to spherical molecules of the same molecular weight. From DLS measurements the translational diffusion coefficient (D) was obtained, while R_H was derived from the Stokes-Einstein equation: $R_H = K \cdot T / 3\pi\eta \cdot D$, where K is the Boltzman constant, T is the absolute temperature, and η is the solution viscosity [20]. Thereafter, the molecular weight was estimated using the Protein Utilities tool of the Zetasizer Nano S software. This tool makes use of a calibration curve obtained by plotting the measured R_H value versus the known molecular weight (M_w) of monomeric and oligomeric globular protein standards in the range 17-1120 kDa. The data points in the calibration curve were fitted with the phenomenological equation $R_H = (a \cdot Mw)^b$, where a and b are fitting parameters. The size distribution of F5 was first analysed according to the per cent intensity of the scattering molecules, yielding a mean radius (z-average) of 11.02 nm with a quite high polydispersivity index (PdI = 0.40) (not shown), suggestive of large conformational heterogeneity of F5 [20]. DLS analysis of F5 is further complicated by the elongated carbohydrate chain(s) accounting for about 14% of P1/P2 molecular weight and protruding outside the protein surface. Considering that at a fixed protein concentration light scattering from large molecules is by far more intense than that from small molecules, the size distribution of F5 was expressed as the per cent volume occupied by the scattering molecules having a certain size. In the latter case, a R_H of 4.91 nm was obtained, with a peak width as large as 2.95 nm (Fig. 5C). The R_H value corresponds to an estimated Mw of 139 kDa, fully compatible with the presence of a P1/P2 hexamer. Nevertheless, the value of peak width limits the possibility to resolve different oligomers having R_H values in the same order of magnitude and is a clear indication of polydisperse size distribution that can arise from the presence of P1/P2 oligomers existing in equilibrium with each other and from conformational heterogeneity introduced by carbohydrate chains.

Altogether, RP-HPLC, SEC and DLS data concurrently suggest that the active fraction F5 is composed of P1 and P2 subunits interacting in a stoichiometric 1:1 ratio to form a tetramer structure in equilibrium with a hexamer form.

Sequencing P1 and P2 subunits of F5 by peptide mass fingerprint analysis

Although P1 and P2 have very close molecular mass and the same number of Cys-residues, they display very different retention time values in RP-HPLC, suggestive of a different amino acid composition or surface charge exposure. This prompted us to undertake the *de novo* sequencing of P1 and P2. HPLC purified P1 and P2, (see Fig. 5A) were subjected to N-terminal sequencing by Edman degradation on a liquid-phase protein sequencer. In both fractions, the sequence HKXEIXHGFGDD was obtained in which X denotes the absence of a well-defined phenylthiohydantoyl amino acid, indicating the presence of a disulfide-bridged Cys in the X position. A BLAST search revealed that the N-terminal sequence HKCEICHGFGDD found in P1 and P2 matched the sequence 1-12, DKCEICHGFGDD, of the secretory phospholypase A2 (sPLA2) inhibitory protein (PIP) isolated from *P. reticulatus* (SwissProt accession number: Q9I8P7) [14], except for an amino acid replacement in position 1 (i.e., His in *P. sebae* instead of Asp in *P. reticulatus*).

Internal sequence information on P1 and P2 were obtained by peptide mass fingerprinting of reduced and S-alkylated proteins with trypsin and Glu-C endoproteinase after RP-HPLC analysis. Proteolytic peptides eluted with the chromatographic peaks in Fig. S3 (Supplemental Data) were collected and their accurate mass determined by ESI-TOF or LTQ-Orbitrap MS (Tables S3 and S4 of Supplemental Data), before and after treatment with N-glycosidase F. Besides accurate MS analysis, Cys-containing peptides were readily identified by the absorbance spectrum of the S-β-(4-pyridylethyl)-moiety, showing a characteristic shape with a maximum at 254 nm [18], by the appearance of a pyridylethyl-fragment ion of 106 a.m.u. in the MS spectrum. In many cases, the chemical identity of proteolytic peptides was also confirmed by MS/MS sequencing on a MALDI-TOF-TOF analysis (see Fig. S4 and Table S5). Notably, some anomalous (e.g., chymotryptic) cleavage was found during proteolysis with trypsin and confirmed by careful MS-MS analysis.

Glycosylation sites were identified by measuring accurate mass values of the proteolytic peptides in Fig S3AB before and after treatment with N-glycosidase F. In the case of P1, the peptide eluting with peak 8 in Fig. S3A has a mass of 4391.5 a.m.u. After deglycosylation, the same peptide has a mass of 1528.8 a.m.u, compatible with the P1 fragment 132-144, EENYAG**NIT**YNIK, (Table S3). Likewise, in the case of P2 the peptide eluting with peak 10 (4419.7 a.m.u.) in Fig. S3B after deglycosylation is converted into a peptide with mass of 1556.8 a.m.u., corresponding to the P2 fragment 132-144, EENYVG**NIT**YNIK, (Table S4). In both cases, a mass difference of 2862 ± 0.8 a.m.u. was measured, in excellent agreement with the value measured after deglycosylation of intact P2 (see above). Noteworthy, using the NetNGlyc on-line server, Asn138 in the NIT sequence of P1 and P2 was identified as a very potent N-glycosylation site. Hence, we conclude that P1 and P2 contain a single glycosylation site at Asn138.

From the data reported in the Supplementary materials and using the amino acid sequence of PIP from *P. reticulatus* as a template (i.e., 182 amino acids) [14], we identified 159 and 177 amino acids in P1 and P2, respectively, corresponding to a sequence coverage of 87.4% and 97.2% (Fig. 6). Assignment of the isobaric Ile or Leu relay on the template sequence of PIP which was deduced from the cDNA sequence [14].

Inhibition of phospholypase activity by F5

Despite high sequence similarity of P1 and P2 with PIP from *P. reticulatus*, F5 exhibited only a modest inhibitory activity on group II sPLA2 from bee venom and on A431-released sPLA2 (Fig. 7A and B). Furthermore, no effect was observed on group V sPLA2 (Fig. 7C).

Conformational Characterization

The conformational properties of purified P1 and P2 were investigated by circular dichroism (CD) in the far-UV region, a spectroscopic techniques that gives information on the type of secondary structure content in proteins [21]. The CD spectra of both P1 and P2 (Fig. 8) share similar features, with a minimum centered at 212-215 nm, typical of proteins containing a predominant β-sheet secondary structure [21].

Discussion

In this work for the first time, we purified from the serum of the non venomous snake *P. sebae*, termed PSS, a protein having a selective anti tumor activity. PSS cytotoxicity was evaluated in cell suspension and in cell adhesion experiments using both tumor and non tumor cell lines. In both experimental conditions and for all the cell lines, PSS exhibited a remarkable and dose-dependent cytotoxic effect. Exposure to low concentration of PSS for prolonged time also affected cell viability as measured by the MTT assay. After exposure to PSS at concentration ranging from 400 to 2000 µg/ml, changes of morphology and cell lysis occurred within minutes. Microscope observation of cells exposed for several hours to PSS, evidenced that a consistent proportion of the cell monolayer became detached. The time dependence of the changes in cell morphology (1 h), is evocative of a rapid treatment-induced gradual loss of cell-matrix adhesion, similar to that documented for other cytotoxic molecules obtained from snakes [22,23]. Consistent with the morphological appearance of cytoplasmic retraction, rounding of cell shape and lysis of cell bodies, PSS effects were mainly associated with cell apoptosis and necrosis. With respect to the decrease in cell viability and the morphological changes observed following exposure to PSS, our data suggest a direct cytotoxic/pro-apoptotic activity of the serum in vitro. A key finding of this work was that the cytotoxic effect appears to be more pronounced on human tumor cells than in non-tumor cells. At concentration of 50 µg/ml PSS was devoid of any effect on non-tumor cell lines, while inducing over 50% inhibition of tumor cell growth. These effects were absent at concentrations lower than 50 µg/ml.

In vivo experiments demonstrated that the cytotoxic effect produced in vitro on tumor cell lines translated in tumor growth inhibition in nude mice bearing epithelial tumors (A431). PSS peritumoral treatment was well tolerated and reduced tumor growth by 20%. Although biased by the limited number of mice that could be studied given the limited availability of the source. Interestingly, we found interesting that the treatment appeared to increase mice survival. Given the limited availability of the natural source (i.e., the python serum, PSS), this finding might be biased by the small number of mice that could be studied. Nevertheless, the effects on tumor growth reduction and increasing mice survival were significant and appeared worthy of further chemical and functional analysis aimed at isolating the active component responsible for the cytotoxic/antitumor activity of PSS.

The active protein component, F5, was purified from the crude serum by ion-exchange chromatography and its antitumor activity assessed on several different tumor cell lines, *in vitro,* and in tumor xenograft, *in vivo*. *In vivo* F5 exhibited potent antitumor effect compared to PSS. Strikingly, after 12-days treatment, we observed a reduction in tumor size of approximately 60%, in comparison with that measured with buffer alone or with the non-cytotoxic F3 fraction (Fig. 3C). Although quite remarkable (Fig. 3B), the cytotoxicity of F5 was not higher than that of the whole python blood serum assayed at the same protein concentration (Fig. 1 and Fig. 3B). The reduction of the specific activity of bioactive proteins purified from natural sources is not rare. In our case, this effect could be accounted for by the different physico-chemical properties (e.g., pH, ionic strength and viscosity) of the python blood serum compared to those of the purification buffer or the assay medium. These differences or the presence of specific ligands (e.g., lipids) in the serum, that are discarded during purification, might affect the oligomerization state of F5, perhaps promoting the formation of large inactive protein aggregates (see Fig. 3A), with a resulting alteration of the biological function.

The data shown in Fig. 4 indicate that F5 reduced tumor cell viability and induced apoptosis by activation of caspase-3 pathway. In an attempt to identify the molecular target of F5, the β-tubulin distribution was measured in cells treated with the active protein component F5, but no effect was observed on microtubule dynamics. Limitations in the supply of the python blood serum prevented a comprehensive assessment of the putative mechanism for the anti-proliferative activity.

These promising results prompted us to undertake a thorough chemical and conformational characterisation of the F5 component. Our data concurrently indicate that F5 is composed of two non-covalently linked protein subunits, P1 and P2, of about 23 kDa each and interacting in a stoichiometric 1:1 ratio to form a predominant heterotetrameric structure existing in equilibrium with a hetero-hexameric form. Importantly, the PIP inhibitor form *P. reticulatus*, displaying high sequence similarity with P1 and P2, forms a homo-hexamer [14]. Each subunit in F5 contains a single carbohydrate chain of approximately 3 kDa, N-linked to the conserved Asn138, and 16 Cys-residues arranged to form eight intrasubunit disulfide bridges. The two subunits display high sequence identity and only six mutations could be identified between P1 and P2 (i.e., Glu17Gln, Asp65Glu, Met69Ile, Asp109Tyr, Ala136Val, Leu153Val) (Fig. 6). As expected, P1 and P2 also share a similar conformation, characterised by a predominant β-sheet secondary structure (Fig. 8). Interestingly, when purified by RP-HPLC and reconstituted in physiological buffer, the isolated P1 and P2 are still folded but completely lack any biological activity, indicating that the cytotoxic/antitumor function of F5 is inherently associated with the formation of a biologically active F5 oligomer. With respect to this point, the sequence coverage reported in this study was higher than 87 and 97% for P1 or P2, respectively. These detailed sequence information will hopefully allow us to isolate, clone and express the gene(s) encoding for P1 and P2 in the python genome, in order to obtain large protein quantities for further structural and functional analyses.

Another interesting point emerging from our study is that, despite the absolute conservation of Cys-residues and the high sequence similarity that P1 and P2 display with PIP from *P. reticulatus* (Fig. 6), F5 has only poor (if any) inhibitory activity toward PLA2s (Fig. 7). This result is even more intriguing if one considers that the peptide that in PIP specify PLA2s inhibition (i.e., ^{59}VDIHVWDGV^{67} and ^{87}PGLPLSLQNG^{96}) [24,25] are also present in P1 and P2 sequences, albeit with a single point mutation in each peptide segment (i.e., Gln94Lys in P1 and P2 and Asp65Glu in P2) (Fig. 6). In both cases, however, mutations involve charged amino acids. In addition, comparison of P1 and P2 sequences with that of PIP reveals that of the eight mutations found in the assigned P1 sequence (i.e., 159 amino acids) four introduce or eliminate an electric charge (i.e., Asp1His, Gln17Glu, Gln94Lys, Gln132Glu), For P2, ten mutations were found out of 177 amino acids assigned. Of these, seven are expected to severely alter the electrostatics or side-chain volume at the mutation site (i.e., Asp1His, Gln94Lys, Asp109Tyr, Gln132Glu, Ala136Val, Pro178Tyr and Ala179Glu). On these grounds, it is not surprising that modification of the surface electrostatic potential of P1 and P2 subunits, caused by mutations, may alter substrate recognition and hinder F5 anti-PLA2 activity.

In conclusion, in this study we have shown that *P. sebae* serum contains a previously unknown specie specific and selective cytotoxic protein component endowed with pro-apototic activity and *in vivo* antitumor effect which could be exploited for the development of novel antitumor strategies.

Acknowledgements

We thank: Drs. Francesco Trimigliozzi and Marco Bonazza Foselli for providing python serum samples; Drs. Concetta Montemurno, Mario Granito, Francesco Stannisci, Fiorenzo Refosco and Angela for the continuous support during the experimentation; We are indebt with Dr. Lucia Morbidelli (Univ. of Siena) for helping with mice experiments and cell culture, Prof. Gabriella Torcia (University of Florence) for helping with FACS analysis. This work was inspired by S. Padre Pio da Pietrelcina and is dedicated to him and his teachings. The authors have no conflicts of interest pursuant to the current work.

Funding
The work was supported by funds from Associazione del Bene (Foggia, Italy), and AIRC (IG10731) (MZ).

REFERENCES

1. Thwin, M.M., and Gopalakrishnakone P. (1998) Snake endovenomation and protective natural endogenous proteins: a mini review of the recent development (1991-1997). Toxicon **36**, 1471-1482
2. Abu-Sinna, G., Esmat, A.Y., Al-Zahaby, A.A., Soliman, N.A. and Ibrahim, T.M. (2003) Fractionation and characterization of Cerastes snake venom and the antitumor action of its lethal and non-lethal fractions. Toxicon **42**, 207-215
3. Petretski, J.H., Kanashiro, M.M., Rodrigues, F.R., Alves, E.W., Machado, O.L. and Kipnis, T.L. (2000) Edema induction by the disintegrin-like/cysteine-rich domains from a Bothrops atrox hemorrhagin. Biochem. Biophys. Res. Commun. **276**, 29-34
4. Oliveira, J.C., de Oca, H.M., Duarte, M.M., Diniz, C.R. and Fortes-Dias, C.L. (2002) Toxicity of South American snake venoms measured by an in vitro cell culture assay. Toxicon **40**, 321-325
5. Schmitmeier, S., Markland, F.S. and Chen, T.C. (2000) Anti-invasive effect of contortrostatin, a snake venom disintegrin, and TNF-alpha on malignant glioma cells. Anticancer Res. **20**, 4227-423
6. Kini, R.M. (2003) Excitement ahead: structure, function and mechanism of snake venom phospholipase A2 enzymes. Toxicon **42**, 827-840
7. Koh, D. C. I., Armugam A., and Jeyaseelan K. (2006) Snake venom components and their applications in biomedicine. Cell. Mol. Life Sci. **63**, 3030–304
8. Ohkura, N., Okuhara, H., Inoue, S., Ikeda, K. and Hayashi, K. (1997) Purification and characterization of three distinct types of phospholipase A2 inhibitors from the blood plasma of the Chinese mamushi, *Agkistrodon blomhoffii siniticus*. Biochem. J. **325**, 527-531
9. Lambeau, G. and Lazdunski, M. (1999) Receptors for a growing family of secreted phospholipases A2. Trends Pharmacol. Sci. **20**, 162-170
10. Faure, G., Villela, C., Perales, J. and Bon, C. (2000) Interaction of the neurotoxic and nontoxic secretory phospholipases A2 with the crotoxin inhibitor from *Crotalus* serum. Eur. J. Biochem. **267**, 4799-4808
11. Dunn, R.D. and Broady, K.W. (2001) Snake inhibitors of phospholipase A2 enzymes. Biochim. Biophys. Acta **1533**, 29-37
12. Ploug, M. and Ellis, V. (1994) Structure-function relationships in the receptor for urokinase-type plasminogen activator. Comparison to other members of the Ly-6 family and snake venom alpha-neurotoxins. FEBS Lett. **349**, 163-168
13. Okumura, K., Inoue, S., Ikeda, K. and Hayashi, K. (2003) Identification and characterization of a serum protein homologous to alpha-type phospholipase A2 inhibitor (PLIα) from a nonvenomous snake, *Elaphe quadrivirgata*. IUBMB Life. **55**, 539-545
14. Thwin, M.M., Gopalakrishnakone, P., Kini, R.M., Armugam, A. and Jeyaseelan, K. (2000) Recombinant antitoxic and antiinflammatory factor from the nonvenomous snake *Python reticulatus*: phospholipase A2 inhibition and venom neutralizing potential. Biochemistry **39**, 9604-9611
15. Donnini, S., Solito, R., Monti, M., Balduini, W., Carloni, S., Cimino, M., Bampton, E.T., Pinon, L.G., Nicotera, P., Thorpe, P.E., Ziche, M. (2009) Prevention of ischemic brain injury by treatment with the membrane penetrating apoptosis inhibitor, TAT-BH4 Cell Cycle **8**, 1271-1278
16. Cantara, S., Thorpe, P.E., Ziche, M., and Donnini, S. (2007) TAT-BH4 counteracts Abeta toxicity on capillary endothelium. FEBS Lett. **581**, 702-706
17. Donnini, S., Finetti, F., Solito, R., Terzuoli, E., Sacchetti, A., Morbidelli, L., Patrignani, P., Ziche, M. (2007) EP2 prostanoid receptor promotes squamous cell carcinoma growth through epidermal growth factor receptor transactivation and iNOS and ERK1/2 pathways. FASEB J. **21**, 2418-2430

18. Moritz, R.L., Eddes, J.S., Reid, G.E. and Simpson, R.J. (1996) S-pyridylethylation of intact polyacrylamide gels and in situ digestion of electrophoretically separated proteins: a rapid mass spectrometric method for identifying cysteine-containing peptides. Electrophoresis **17**, 907-917
19. Corbett, R.J., and Roche, R.S. (1984) Use of high-speed size-exclusion chromatography for the study of protein folding and stability. Biochemistry **23**, 1888-1894
20. Harding, S.E., and Jumel, K. (2004) Light scattering in *Current Protocols in Protein Science* (Coligan J.E., Dunn, B.M. et al., Eds.). John Wiley, New York, USA.
21. Brahms, S., and Brahms, J. (1980) Determination of protein secondary structure in solution by vacuum ultraviolet circular dichroism. J. Mol. Biol. **138**, 149-178
22. Baramova, E.N., Shannon, J.D., Bjarnason, J.B., and Fox, J.W. (1989) Degradation of extracellular matrix proteins by hemorrhagic metalloproteinases. Arch. Biochem. Biophys. **275**, 63-71
23. Coelho, A.L., de Freitas, M.S., Oliveira-Carvalho, A.L., Moura-Neto, V., Zingali, R.B., and Barja-Fidalgo, C. (1999) Effects of jarastatin, a novel snake venom disintegrin, on neutrophil migration and actin cytoskeleton dynamics. Exp. Cell. Res. **251**, 379-387
24. Thwin, M.M., Satish, R.L., Chan, S.T., and Gopalakrishnakone, P. (2002) Functional site of endogenous phospholipase A2 inhibitor from python serum. Eur. J. Biochem. **269**, 719-727
25. Thwin, M.M., Satyanarayanajois, S.D., Nagarajarao, L.M., Sato, K., Arjunan, P., Ramapatna, S.L., Kumar, P.V., and Gopalakrishnakone, P. (2007) Novel peptide inhibitors of human secretory phospholipase A2 with antiinflammatory activity: solution structure and molecular modeling. J. Med. Chem. **50**, 5938-5950

Biochemical Journal Immediate Publication. Published on 12 Aug 2011 as manuscript BJ20100739

Table 1: Effect of PSS on cell death

PSS [µg/ml]	A431 Apoptosis (% cell Annexin V positive)	A431 Necrosis (% cell PI positive)	U373MG Apoptosis (% cell Annexin V positive)	U373MG Necrosis (% cell PI positive)
0	9 ± 3	10 ± 4	7 ± 2	8 ± 2
25	8 ± 1	8 ± 2	7 ± 3	27 ± 3**
50	8 ± 3	15 ± 4	7 ± 5	44 ± 11**
100	23 ± 6**	45 ± 5**	24 ± 7**	48 ± 9 **

Apoptosis (Annexin V positive cells) and necrosis (Propidium iodide positive cells) were measured by FACS analysis after 4 h exposure of A431 and U373MG cell lines to different concentration of PSS. Data ± SD are expressed as % of positive cells for annexin V or propidium iodide of three experiments run in triplicate. **p<0.01, ***p<0.001 vs basal (0 µg/ml PSS).

FIGURE LEGENDS

Figure 1. Effect of PSS on cell viability. A panel of tumor and non tumor cells was used: coronary venular endothelial cell (CVEC), human fibroblast (HF), human breast carcinoma cells (MCF-7), human glioblastoma cells (U373MG), human squamous cell carcinoma (A431). Cell viability was quantified by MTT assay after 5 days exposure to 10-25-50 µg/ml. Data are expressed as % cell viability and are the mean of three experiments run in triplicate. Basal = 1% FCS. *p<0.05 vs basal, **p<0.01 vs basal, ***p<0.001 vs basal.

Figure 2. Effect of PSS on A431 tumor growing subcutaneously. A431 cells (10^6/mouse) were injected subcutaneously (s.c.) in Balb/c nude mice (day 0). PSS (100 µg/100 µl) or vehicle (PBS, 100 µl), was injected every other day s.c. close to the tumor mass. Tumor volumes are reported as mean ± SEM, n = 6, *P<0.05 vs vehicle. TI = Tumor Injection.

Figure 3. Fractionation of PSS and effect of F1-F6 fractions on *in vitro* tumor cell viability, and *in vivo* tumor growth. **A.** Fractionation of PSS by anion-exchange chromatography. An aliquot (140 µl) of PSS was loaded onto a Mono-Q analytical column, equilibrated in 20 mM Tris-HCl pH 7.5, containing 0.15 M NaCl at a flow rate of 0.5 ml/min, and eluted with a linear gradient of NaCl from 0.15 to 1.0 M. All fractions were subjected to analysis of total protein content and then tested for cytotoxic antitumoral activity. Inset, SDS-PAGE (12% acrylamide) of protein fractions eluted from the ion-exchange column. S*, low molecular weight protein standard mixture; PSS, crude serum (0.5 µl) from *P. sebae*; fractions F2-F5 (5 µg/20 µl each) as reported in Fig. 3A. **B**. Eluted fractions (F1 to F6) were tested for their effects on tumor cells. Cell viability was monitored by TB exclusion after 1-h treatment and MTT test after 48-h treatment. MTT data are expressed as % cell viability and are the mean of at least two experiments run in triplicate. TB data are expressed as % dead cells/total cell counted. Control = 10% FCS. *p<0.05 vs control. **C.** A431 cells (10^6/mouse) were injected subcutaneously (s.c.) in Balb/c nude mice. F5 (50 µg/100 µl) or F3 (50 µg/100 µl) or vehicle (PBS, 100 µl), were injected every other day s.c. close to the tumor mass. Tumor volumes are reported as mean ± SEM, n = 6, *P<0.05 vs vehicle.

Figure 4. F5 induces cell apoptosis. **A.** Western blot analysis of cleaved caspase-3 in response to F1 and F5 (50 µg/ml, 24 h). Actin was used for normalization. The graph represents the quantification of gels (ADU = arbotrary densitometric analysis). Gels are representative of three experiments with similar results. **B.** Phosphatidylserine expression on A431 exposed for 24 h to F1 or F5 (50 µg/ml) in 1% FCS (Control). Magnification 40x.

Figure 5. Chemical characterization of F5. A. RP-HPLC analysis of F5. An aliquot (20 µg) of F5 was loaded onto a Vydac (4.6 x 150 mm) C4 column eluted with a linear acetonitrile/0.1%TFA gradient (---) at a flow rate of 0.8 ml/min. Two peaks, named P1 and P2, were eluted at 19 and 25 min, respectively, were then collected and subjected to peptide mass fingerprint analysis. **B.** Size-exclusion chromatography of F5. F5 aliquots (100 µl) eluted from ion-exchange chromatography (Fig. 3A) were loaded onto a Supersose-12 column eluted at a flow rate of 0.3 ml/ml and calibrated with suitable protein standards (Inset). **C.** Dynamic light scattering analysis of F5. Measurements were carried out at 25 °C at a protein concentration of 0.7 mg/ml. Size distribution is expressed as the per cent volume occupied by molecules with a certain size.

Figure 6. Sequence alignment of P1 and P2 from *P. sebae* with PIP from *P. reticulatus*. In green are indicated the amino acids of P1 and P2 that are different in PIP. The peptide segments of PIP that could not be identified in P1 and P2 are indicated in gray.

Figure 7. Effect of F5 on PLA2 activity. **A.** The effect of F5 was evaluated on group II PLA2 enzyme activity derived from bee venom (BV) or from PLA2 enzyme activity released by A431 cultured for 24 h in 10% FCS. **B**. The effect of F5 was measured by using the sPLA2 Assay Kit and evaluated by measuring the bsorbance at 405 nm. **C.** Effect of F1, F5 or PSS on group V sPLA2 enzyme activity. The inhibitory activity of PSS or its fractions was assayed by the sPLA2 (type V) Inhibitor Screening Assay kit and measured as in panel B. Data are reported as % inhibition for each sample versus sPLA2 activity reported as 100%.

Figure 8. Far-UV circular dichroism (CD) of P1 and P2. CD spectra were of P1 and P2 were recorded in 10 mM sodium phosphate, pH 7.0 at a protein concentration of 0.17 mg/ml for both proteins. Ellipticity data are expressed in millidegrees without further normalisation.

Figure 1

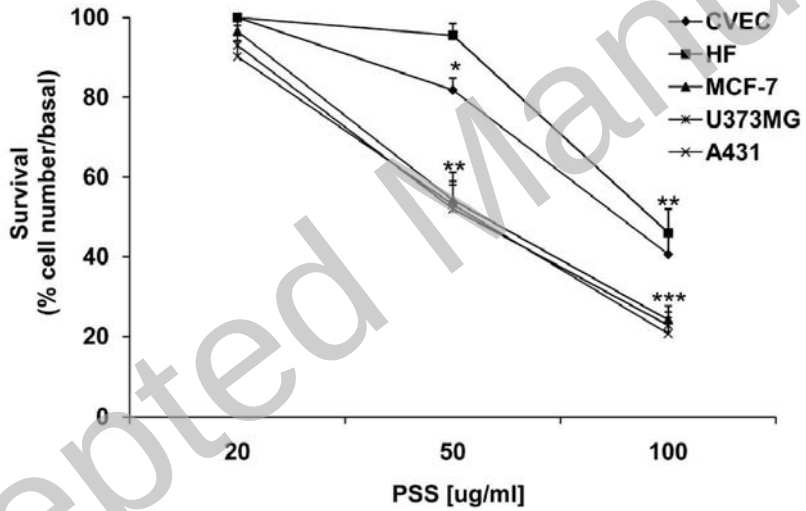

Figure 2

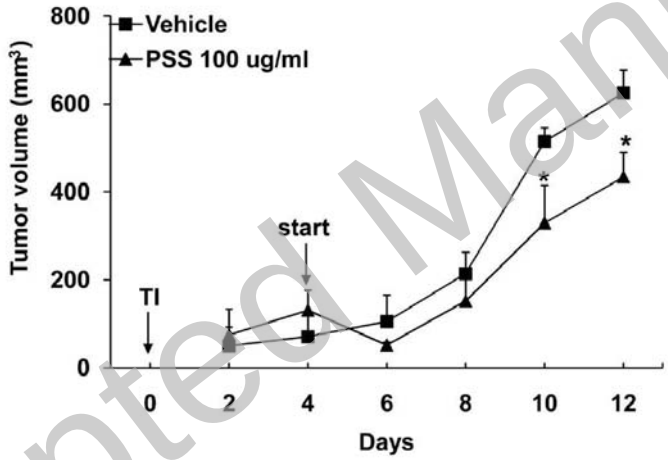

Figure 3

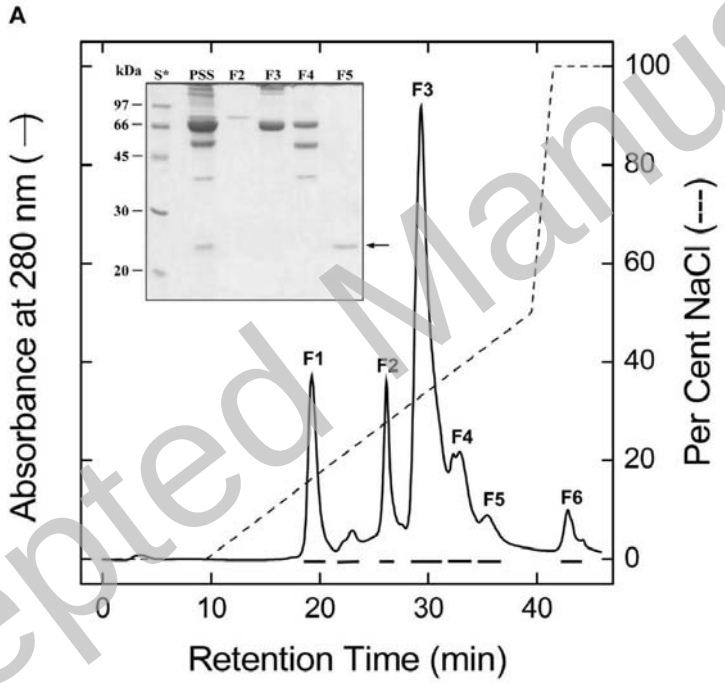

B

	Survival (% Cell Viability)			% Dead cells/Total cells counted		
	A431	MCF-7	U373MG	A431	MCF-7	U373MG
Control	100	100	100	1.4 ± 1.6	2.4 ± 2	3.2 ± 3
F1	119 ± 9			2.2 ± 1.9		
F2	97 ± 20			4 ± 2.7		
F3	90 ± 10	87 ± 15	94 ± 12	3 ± 2.7	2.9 ± 1.7	4.7 ± 4
F4	84 ± 6 *			8 ± 1.7 *		
F5	63 ± 4 **	53± 3 **	58 ± 5 **	14 ± 4 *	21 ± 3.4 *	18 ± 5 *
F6	100 ± 3			2.3 ± 2.9		

C

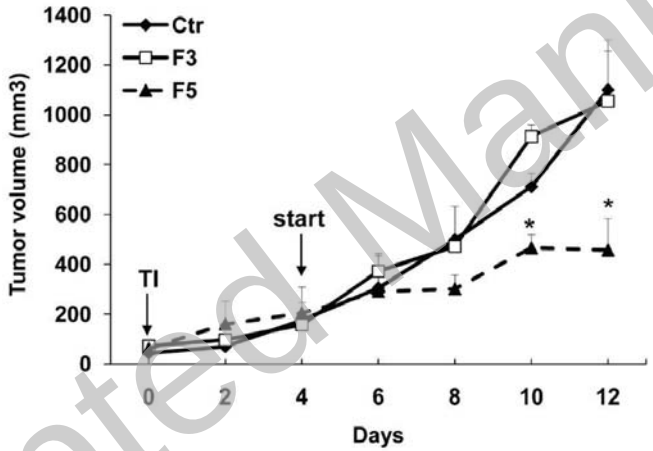

Figure 4

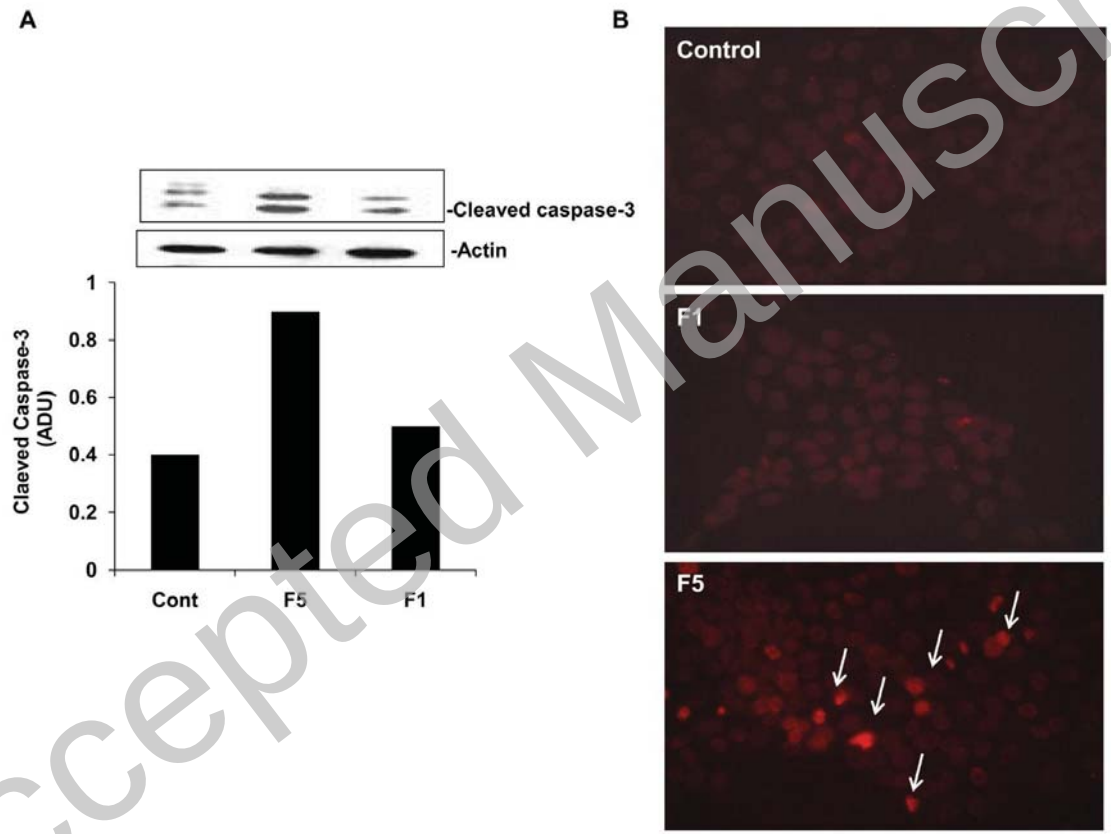

Biochemical Journal Immediate Publication. Published on 12 Aug 2011 as manuscript BJ20100739

Figure 5

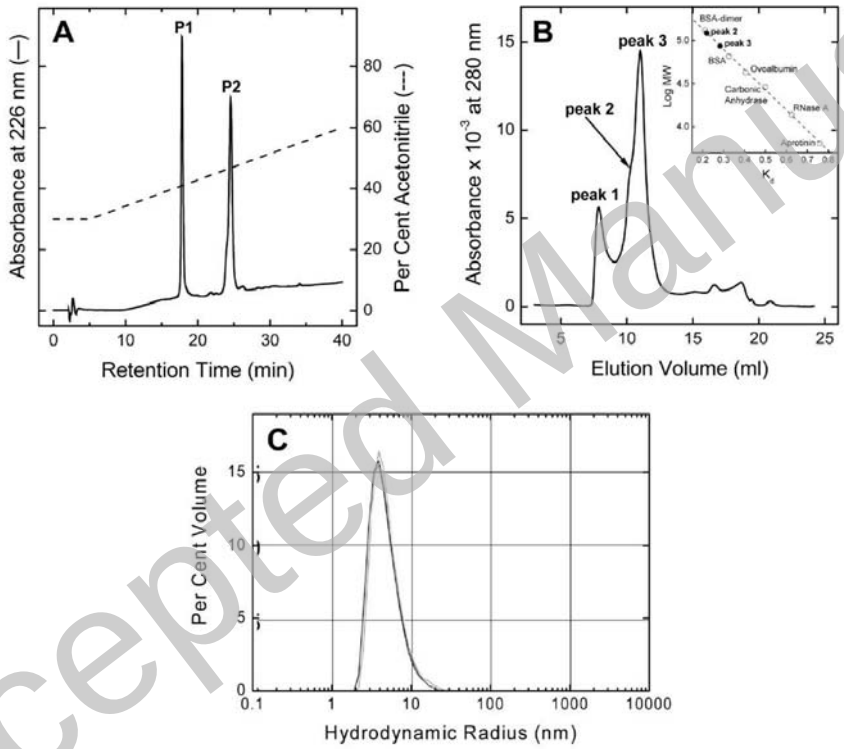

Biochemical Journal Immediate Publication. Published on 12 Aug 2011 as manuscript BJ20100739

Figure 6

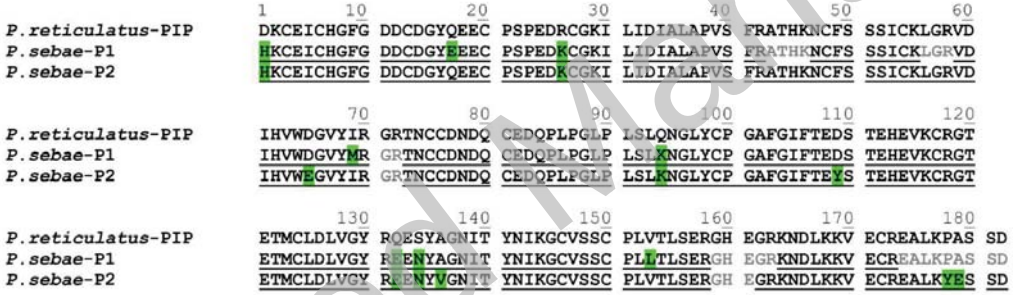

Biochemical Journal Immediate Publication. Published on 12 Aug 2011 as manuscript BJ20100739

Figure 7

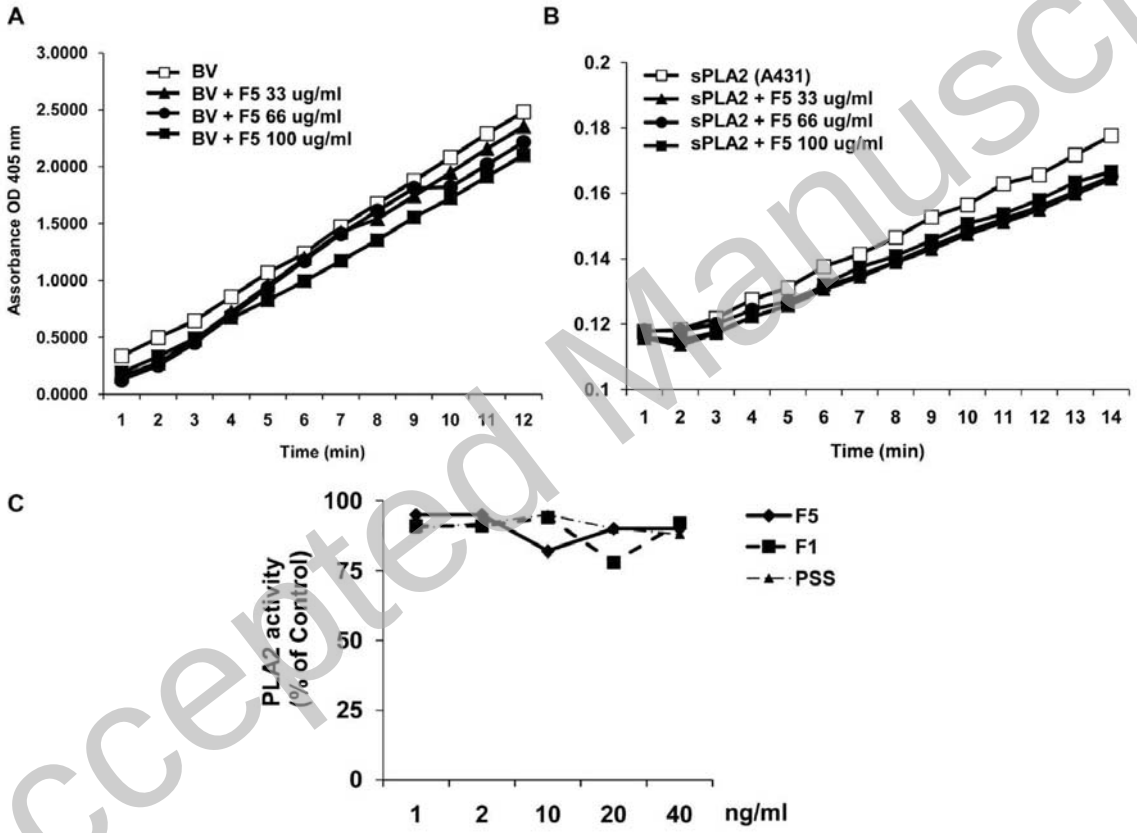

Figure 8